Research Article

Fabrication and *In Vitro* Evaluation of Nanosized Hydroxyapatite/Chitosan-Based Tissue Engineering Scaffolds

Tao Sun,[1] Tareef Hayat Khan,[2] and Naznin Sultana[3]

[1] *Miniaturized Medical Devices Program, Institute of Microelectronics, Agency for Science, Technology and Research (A * STAR), Singapore 117685*
[2] *KALAM, Faculty of Alam Bina, Universiti Teknologi Malaysia, 81310 Johor Bahru, Malaysia*
[3] *Faculty of Biosciences and Medical Engineering, Universiti Teknologi Malaysia, 81310 Johor Bahru, Malaysia*

Correspondence should be addressed to Naznin Sultana; naznin@biomedical.utm.my

Composite scaffolds based on biodegradable natural polymer and osteoconductive hydroxyapatite (HA) nanoparticles can be promising for a variety of tissue engineering (TE) applications. This study addressed the fabrication of three-dimensional (3D) porous composite scaffolds composed of HA and chitosan fabricated via thermally induced phase separation and freeze-drying technique. The scaffolds produced were subsequently characterized in terms of microstructure, porosity, and mechanical property. *In vitro* degradation and *in vitro* biological evaluation were also investigated. The scaffolds were highly porous and had interconnected pore structures. The pore sizes ranged from several microns to a few hundred microns. The incorporated HA nanoparticles were well mixed and physically coexisted with chitosan in composite scaffold structures. The addition of 10% (w/w) HA nanoparticles to chitosan enhanced the compressive mechanical properties of composite scaffold compared to pure chitosan scaffold. *In vitro* degradation results in phosphate buffered saline (PBS) showed slower uptake properties of composite scaffolds. Moreover, the scaffolds showed positive response to mouse fibroblast L929 cells attachment. Overall, the findings suggest that HA/chitosan composite scaffolds could be suitable for TE applications.

1. Introduction

The development of three-dimensional (3D) scaffold which can provide an appropriate microenvironment for tissue growth and regeneration is required by tissue engineering (TE) [1, 2]. TE aims at finding biodegradable and biocompatible scaffolds that can be seeded with cells for both *in vitro* and *in vivo* purposes [3]. One of the major objectives of the scaffolds is to mimic the natural characteristics of extracellular matrix (ECM). The appropriate scaffold architecture is vital to allow vascularization and to supply adequate nutrients to the developing tissue. Therefore, scaffolds must possess some special features, such as an appropriate surface chemistry, biodegradability, nontoxicity, an interconnected porous network, appropriate pore size, and shape to attain sufficient nutrient transport and cell in-growth [4, 5].

Thermally induced phase separation (TIPS) of polymer solution was reported to be used in the field of drug delivery and to fabricate microspheres in order to incorporate biological and pharmaceutical agents [6, 7]. In order to fabricate tissue engineering scaffolds, this process has become much more popular. By altering the types of polymer and solvent, polymer concentration, and phase separation temperature, different types of porous scaffolds with micro- and macrostructured scaffolds can be produced. In order to control pore morphology on a micrometer to nanometer level, TIPS process can be utilized [6]. In this technique, firstly, the polymer is dissolved in a solvent, and then the bioactive molecule is dissolved or dispersed in the resulting homogeneous solution, which is then cooled in a controlled fashion until solid-liquid or liquid-liquid phase separation is induced. The resulting bicontinuous polymer and solvent phases are

then quenched to create a two-phase solid. By sublimation, solidified solvent is then removed, leaving a porous polymer scaffold with bioactive molecules incorporated within the polymer. To incorporate small molecules into the polymer scaffolds, this technique is useful.

Chitosan is one of the most common natural biopolymers used for bone tissue engineering [8–10]. Natural polymers can possess highly organized structure to guide cells to grow and may stimulate an immune response at the same time. Being a linear polysaccharide, chitosan is composed of glucosamine and N-acetyl glucosamine units. Due to several properties such as tissue compatibility, bioresorbability, antibacterial activity, and haemostatic characteristics, chitosan is a suitable material for biomedical applications [11]. Moreover, the degradation products of chitosan are nontoxic, nonimmunogenic, and noncarcinogenic [12]. On the other hand, hydroxyapatite (HA) is a frequent choice and possesses osteoconductive properties which demonstrated excellent cellular and tissue responses *in vitro* and *in vivo*. Together with biocompatibility, HA has chemical structures similar to bone minerals and has been used in bone graft, augmentation, and substitution [13–16].

In this study, chitosan and HA/chitosan scaffolds were fabricated with desired pore sizes and porosity using thermally induced phase separation technique. In a second step, the scaffolds were characterized using various methods. The *in vitro* degradation and the response of fibroblast cells on porous chitosan-based scaffolds were also evaluated.

2. Materials and Methods

2.1. Materials. Chitosan with medium molecular weight and in the powder form was purchased from Sigma-Aldrich. 2% (v/v) acetic acid solution was prepared using glacial acetic acid in ultrapure milliQ water. The HA nanoparticles were produced via a nanoemulsion process [17].

2.2. Fabrication of Chitosan Scaffolds. The thermally induced phase separation technique was used to fabricate the scaffold. Firstly, 0.5 g of chitosan was weighed accurately into a centrifuge tube. Then, an accurately measured amount of 2% acetic acid was added to the centrifuge tube to make an emulsion. The mixtures were homogenized using a homogenizer (Ultra-Turrax, IKAWERKE, Germany) at a fixed speed. The homogeneous solution was put into a capped glass tube and frozen in a freezer at a preset temperature of −18°C for 24 hour. The frozen samples were then freeze dried for 72 hour in freeze-drying vessel (LABCONCO-Freeze dry system, USA) to remove the solvent completely. The scaffolds produced were stored in a desiccator until it is used for characterization.

2.3. Fabrication of HA/Chitosan Scaffolds. The HA/chitosan composite scaffolds were also fabricated using the thermally induced phase separation technique. The HA nanoparticles were weighed accurately and added to the centrifuge tube containing 0.5 g of chitosan polymer. Then, 20 mL of 2% (v/v) acetic acid was added, homogenized using the homogenizer (Ultra-Turrax, IKAWERKE, Germany), and transferred into

a freezer at a preset temperature in capped glass tubes. The solidified solution was maintained overnight and then was transferred into a freeze-drying vessel (LABCONCO-Freeze dry system, USA) for several days to remove the solvent. Thus, HA/chitosan porous scaffolds were obtained and stored in a desiccator until it is used for characterization.

2.4. Characterization. The cylindrical porous scaffolds were cut into specimens with the size of 15 mm in diameter and 1.5 mm in height using a sharp razor blade. The morphology of the scaffolds was studied using a scanning electron microscope (SEM: Hitachi TM 3000). The presence and distribution of HA nanoparticles in the HA/chitosan composite scaffolds were analyzed by energy dispersive X-ray (EDX) spectrometry.

Using the liquid displacement method, the density and porosity of the scaffolds were measured [18, 19]. Using an Instron mechanical tester (Instron 5848, USA), the compressive mechanical properties of the scaffolds were determined at a crosshead speed of 0.5 mm/min with 100 N load cell.

2.5. In Vitro Degradation. The specimens of diameter (10 mm) and height (1.5 mm) were cut from chitosan and 10% (w/w) HA incorporated HA/chitosan composite scaffolds fabricated from 2.5% polymer solution and weighed. Phosphate buffered saline (PBS) was prepared by dissolving PBS (supplied by Sigma) with distilled water. The specimens were placed in sealable vials containing 10 mL of PBS solution (pH 7.4) and PBS solution was replaced with new solution each week. The samples from PBS were removed at regular intervals, rinsed with distilled water, and dried using a freeze dryer and weighed. The experiment was performed for 4 weeks.

Weight loss during investigation was determined as

$$\text{Weight loss (\%)} = \frac{\left(W_i - W_f\right)}{W_i} \times 100, \tag{1}$$

where W_i and W_f are specimen weights before and after soaking in PBS.

The water uptake was calculated using the following equation:

$$\text{Water uptake (\%)} = \frac{\left(W_w - W_d\right)}{W_d} \times 100, \tag{2}$$

where W_d and W_w are specimen weights before and after soaking in PBS.

2.6. Cell Culture. Based on ISO 10993-5: 2009, a mouse fibroblast cell line (L929, ATCC, USA) was used to evaluate the cytotoxicity of HA/chitosan composite scaffolds. L929 cells were cultured in Eagle's Minimum Essential Medium (EMEM, ATCC 30-2003, USA) containing 10% (v/v) horse serum and incubated at 37°C in an atmosphere of 5% CO_2 and 95% humidity. When the cells were grown to 70–80% confluence, they were detached by 0.25% (w/v) trypsin-ethylenediaminetetraacetic acid (trypsin-EDTA) (Invitrogen Co., USA) and counted by an automated cell counter (Luna, Logos Biosystems, USA).
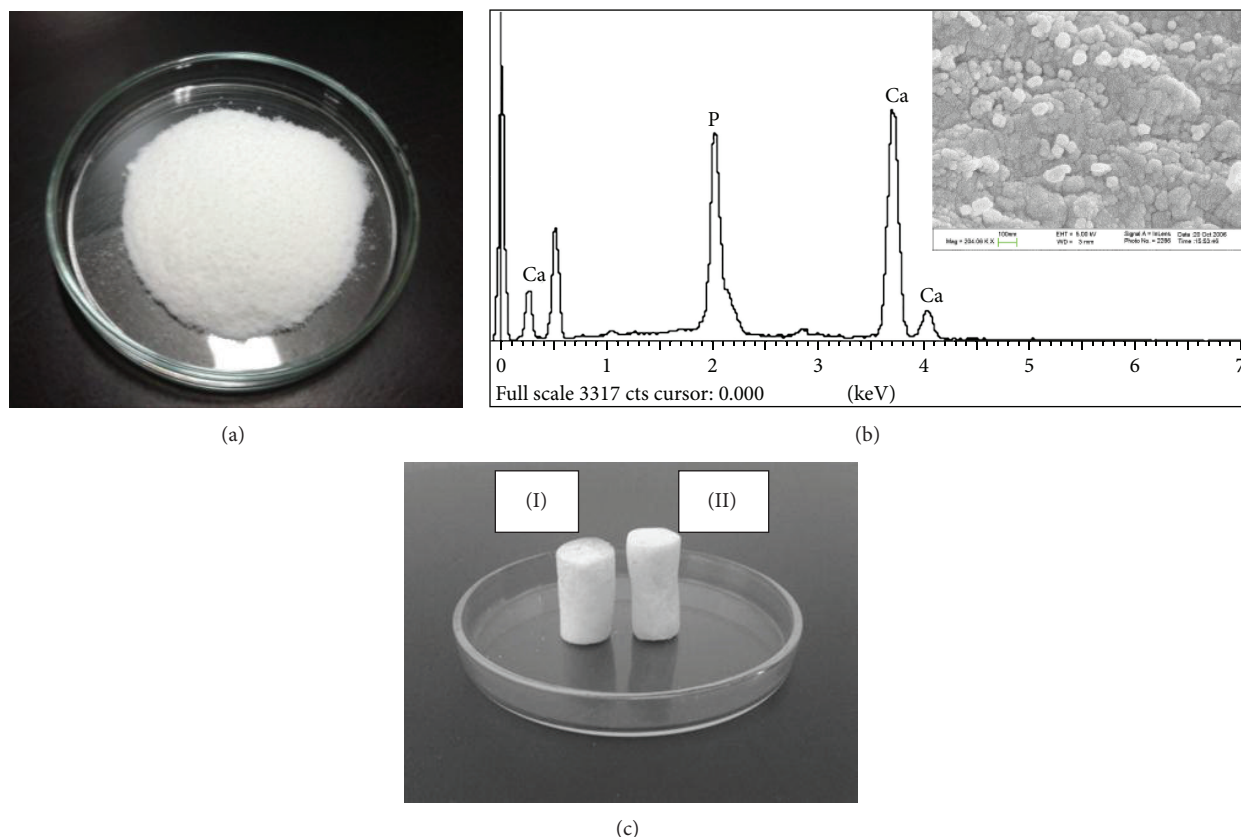
(a)

Full scale 3317 cts cursor: 0.000   (keV)

(b)

(c)

FIGURE 1: General appearance of (a) HA nanoparticles; (b) FESEM and EDX of HA nanoparticles; (c) chitosan (I) and HA/chitosan (II) scaffolds.

2.7. Cell Morphology. L929 cells were cultured at the concentration of 1×10^5 cells/well on 10% (w/w) HA incorporated HA/chitosan composite scaffolds, and then the 24-well cell culture plate containing samples was incubated at 37°C in an atmosphere of 5% CO_2. After 7 days of cell culture, the morphology of cells seeded on the composite scaffolds was observed using SEM. The cells were washed, fixed, dehydrated, and dried prior to SEM examination.

2.8. Live/Dead Assay. In order to determine the viable and nonviable L929 cells adhering to the composite scaffolds after 7 days of culture, live/dead cell staining (live/dead viability/cytotoxicity kit, Invitrogen Co., USA) was performed [20]. Briefly, living cells were stained in green through the enzymatic conversion of the virtually nonfluorescent cell-permeant calcein-AM to the intensely fluorescent calcein (excitation/emission, ∼495 nm/∼515 nm). EthD-1 entered cells with damaged membranes and after binding to nucleic acids produced a bright red fluorescence in dead cells (excitation/emission, ∼495 nm/∼635 nm). After 7 days of culture, L929 cells stained in green and red were observed using a fluorescence microscope (Olympus BX61, Olympus Optical Co., Japan). Cell viability was calculated by counting the number of live cells as well as dead cells and then dividing the number of live cells by the number of total cells. At least 7 areas were randomly chosen for the cell viability assessment.

2.9. Statistical Analysis. All data were presented as mean ± standard deviations (SD). To test the significance, an unpaired Student's *t*-test (two-tail) was applied and a value of $P < 0.05$ was considered to be statistically significant.

3. Results and Discussion

Figure 1(a) shows freeze-dried HA nanoparticles produced in-house using a nanoemulsion process [17]. Figure 1(b) shows the EDX and SEM micrograph of HA nanoparticles. The freeze-dried HA powders used in this investigation consisted of tiny agglomerates of HA nanocrystallites. The particle size of the HA powders was found to be in the range of 20 to 30 nm. From EDX elemental analysis, it was observed that the Ca/P ratio was 1.63 which proves that the HA nanoparticles are calcium deficient. Figure 1(c) represents scaffolds samples produced through thermally induced phase separation process. The scaffolds were relatively large in size and homogeneous in appearance. They could be handled easily and normally did not contain voids (namely, macropores with sizes greater than 1 mm). The scaffolds fabricated had a nonporous thin skin layer. Figure 1(d) shows the specimen that was used for the characterization purposes. Figure 2 is the SEM micrographs, revealing the porous structure of the interior of a scaffold sample. The processing parameters were found to have significant influence on the quality of chitosan
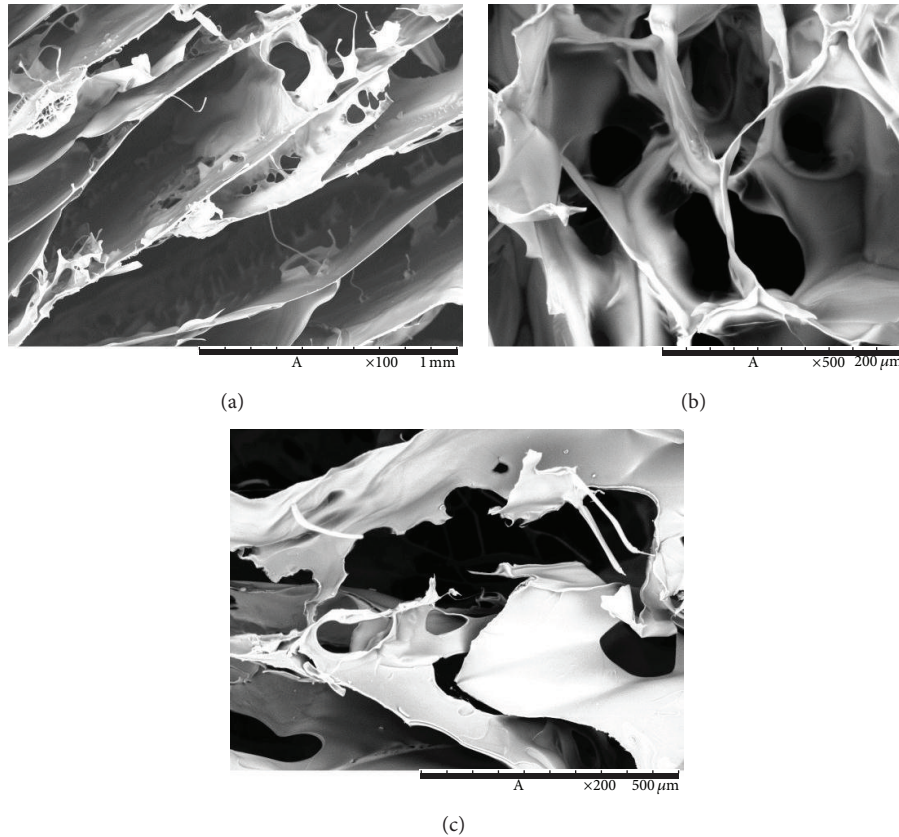
(a)

(b)

(c)

FIGURE 2: SEM micrographs of chitosan scaffolds fabricated with different chitosan concentrations: (a) 2%, (b) 2.5%, and (c) 3.3%.

scaffolds. From the microstructure examination by SEM, it was observed that the concentration of polymer solution had a large effect on the morphology of the scaffold. The effect of polymer concentration on scaffold pore sizes and pore walls was evaluated. Scaffolds produced from solutions at the 2% (w/v) chitosan concentration had thin pore walls and exhibited weak structures (Figure 2(a)). Concentration higher than 3.3% (w/v) possessed high viscosity, which ultimately prevented adequate homogenization. Scaffolds produced from 3.3% (w/v) chitosan solution exhibited thick pore walls with smaller pore sizes (Figure 2(c)). Scaffolds produced from 2.5% (w/v) chitosan concentration had better porous structures (Figures 2(b) and 3). At this concentration, porous structures were obtained with pore sizes over few hundred microns and reasonable thickness of pore walls (Figure 3).
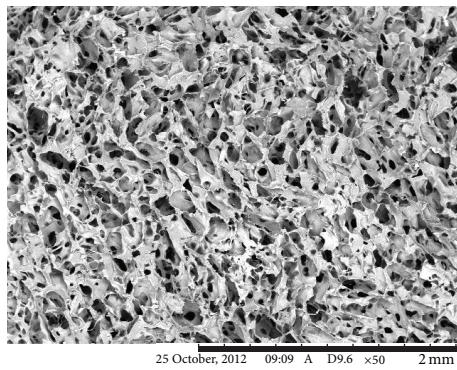
Figure 4 shows SEM micrographs of HA/chitosan composite scaffold. With the incorporation of 10% of HA shown in Figure 4, the porous structure of the composite scaffolds did not change significantly. Compared to the pure chitosan scaffolds, the pore sizes of composite scaffolds decreased slightly. It was observed that good distribution and good adhesion of HA nanoparticles in the chitosan matrix were present. Tiny agglomeration of HA was observed in the polymer pore walls. It was also observed that homogenizing at high speed reduced the agglomeration and helped the HA nanoparticles to disperse well in the polymer pore walls. The EDX analyses at the different locations of composite scaffolds

TABLE 1: The density, porosity, pore type, and compressive modulus of the scaffolds.

Scaffolds (w/v)	Density (g/cm^3)	Porosity (%)	Pore Type	Compressive modulus (MPa)
Chitosan	0.1783	88	Open	1.1 ± 0.2
10% HA/chitosan	0.2918	82	Open	2.8 ± 0.5

confirmed the presence of HA particles well mixed on the polymer pore walls (Figure 4).

Chitosan and HA/chitosan scaffolds with high porosity were fabricated using 2.5% (w/v) chitosan concentrations. With the incorporation of HA scaffolds density increased from 0.1783 g/cm^3 to 0.2918 g/cm^3 and the porosity decreased from 88% to 82% (Table 1). The pores remained open for both chitosan and HA/chitosan scaffolds. The pore sizes ranged from 20 to 350 μm. Another investigation that used a different polymer reported that, by careful selection of different processing parameters, the pore sizes and the thickness of pore walls can be controlled [15, 21, 22]. The formation of porous structure depends on the crystallization of the solvent phase when the solution temperature was lowered. During the phase separation at lower temperature, polymer phase was excluded from the solvent crystallization front and a continuous polymer-rich phase was formed. After the sublimation
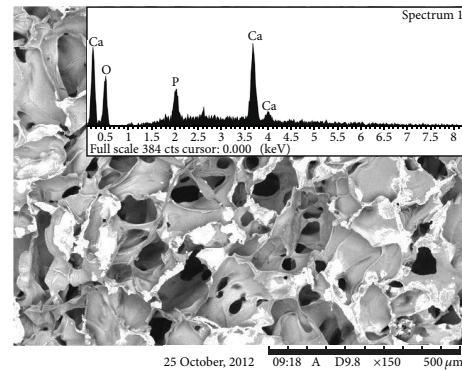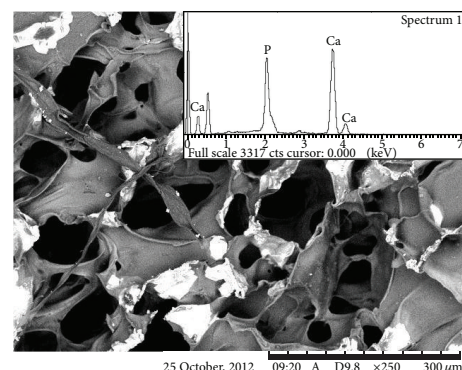
(a)
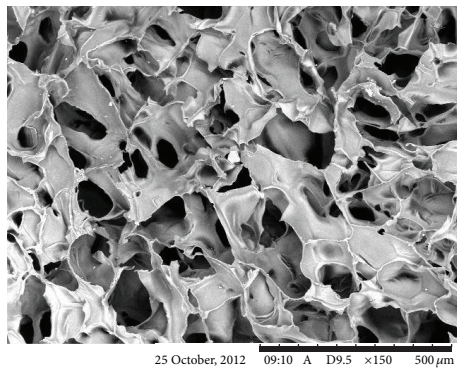
(b)
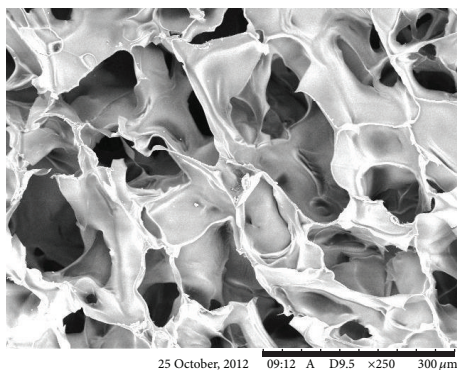
(c)

Figure 3: SEM micrographs of chitosan scaffold at different magnification fabricated from 2.5% chitosan concentration.

(a)

(b)

Figure 4: SEM micrographs and EDX spectra of HA/chitosan composite scaffolds.
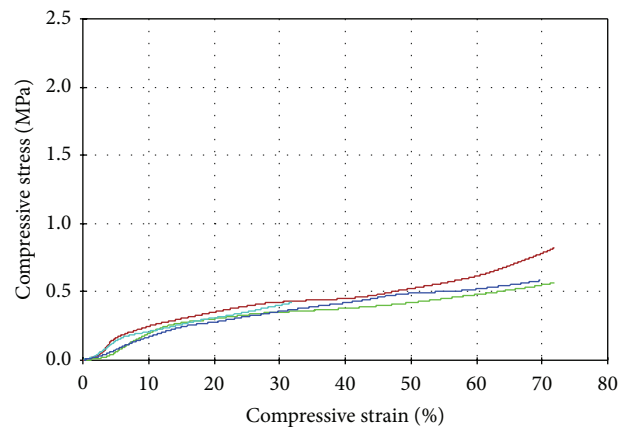
Figure 5: Compressive stress-strain curves of HA/chitosan scaffold.

of solvent phase, scaffolds were formed with the pores of the same geometry of the solvent crystals. Similar phenomenon was also observed when the composite scaffolds were fabricated. Compressive properties of chitosan scaffolds increased with incorporation of HA nanoparticles. In the 2.5% to 7.5% strain range, scaffolds from 2.5% (w/v) chitosan scaffold had a compressive modulus of 1.1 MPa whereas composite scaffolds fabricated from 10% (w/w) HA incorporated 2.5% (w/v) chitosan scaffold had a compressive modulus of 2.8 MPa (Table 1). Figure 5 displays the compressive stress-strain curves of HA/chitosan scaffolds which exhibits three regions, namely, initial linear elasticity, long plateau, and densification region, as observed commonly for "cellular structure" or

porous structure [23]. From the initial linear elasticity, the compressive modulus was calculated. As the HA/chitosan composite scaffolds had higher relative density, it had higher compressive modulus than that of pure chitosan scaffolds.

Figure 6(a) shows the comparison of the water uptake curves between chitosan scaffold and 10% HA in chitosan composite scaffolds at 37°C. It was observed that the initial water uptake of polymer scaffold was much higher than that of composite scaffold as chitosan is well known as hydrophilic
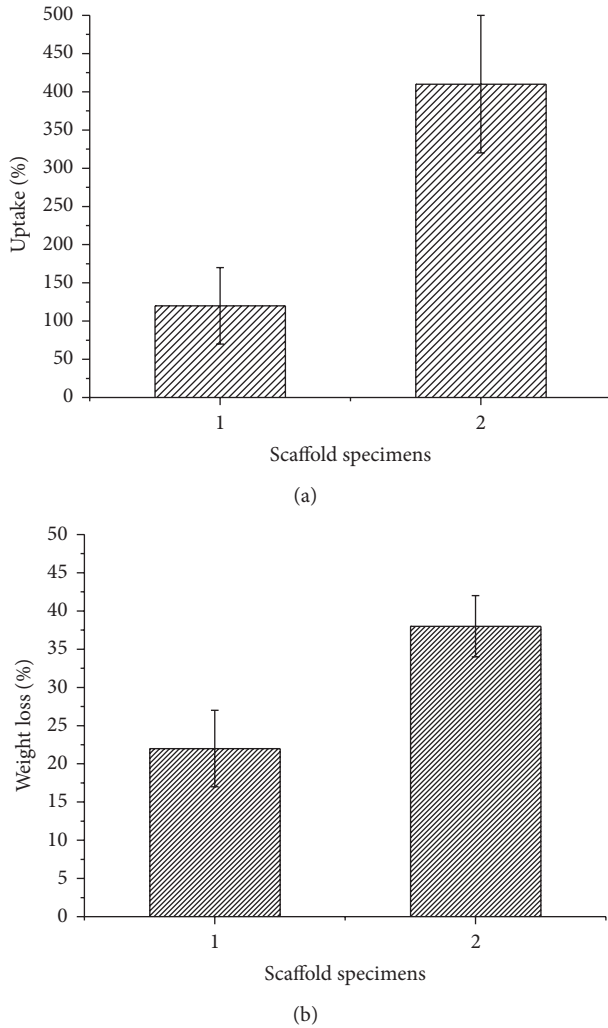
(a)

Figure 6: (a) Uptake of (1) HA/chitosan and (2) chitosan scaffolds; (b) weight loss of (1) chitosan and (2) HA/chitosan scaffolds after *in vitro* degradation for 4 weeks.

25 June, 2012 10:55 A L D5.3 ×100 1 mm

(a)

25 June, 2012 11:14 A L D5.9 ×100 1 mm

(b)

Figure 7: SEM micrographs of (a) chitosan and (b) HA/chitosan scaffolds after *in vitro* degradation for 4 weeks.

polymer. The water uptake of pure chitosan scaffold was about 400% on the other hand the water uptake of HA/chitosan composite scaffold was about 125%. The addition of HA nanoparticles reduced the water uptake properties in the composite scaffolds by stiffening the matrix. The uptake properties were not only related to the degree of porosity as the microstructure of porous matrix may also have an important role. It was reported that the pore size and pore geometry also influenced water uptake [24]. Figure 6(b) displays the weight loss of the scaffold specimens of chitosan (2.5% w/v) and the same composition containing 10% HA over 4-week period of time. After four weeks, the 10% HA containing chitosan composite scaffold showed elevated weight loss (approximately 38%) more than polymer scaffolds (21%). Accelerated weight loss of HA/chitosan composite scaffolds was mainly due to dissolution of HA in the scaffolds matrix.

Figures 7(a) and 7(b) show the morphology of chitosan and HA/chitosan scaffolds after *in vitro* degradation in PBS at 37°C for 4 weeks. Large pores were observed in the chitosan
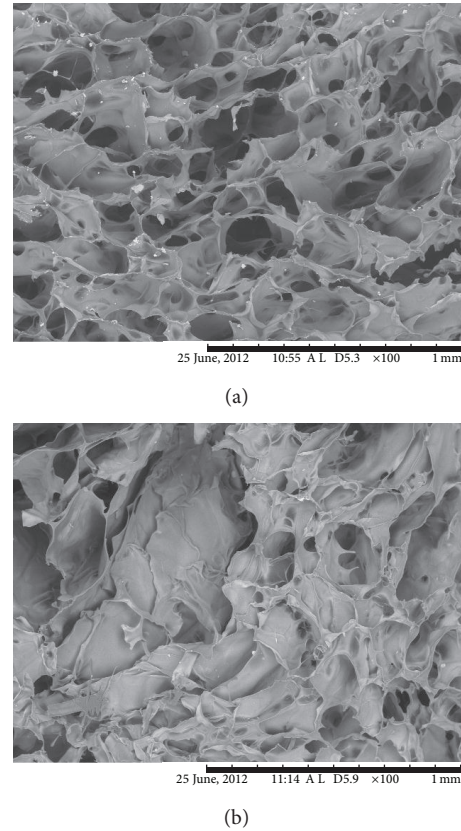
scaffolds after four weeks (Figure 7(a)). Figure 7(b) shows the morphological changes of HA/chitosan composite scaffolds containing 10% of HA after degradation tests. The pore distribution was found to be more irregular after 4 weeks in PBS. Some major morphological changes were detected for composite scaffolds after immersion in PBS for 4 weeks including the elongated and large pores and collapsed pore walls. It was not observed in the pure polymer scaffolds.

In this investigation, tissue culture polystyrene (TCP) and latex plates (10 mm × 10 mm) were used as the negative and positive control groups, respectively. L929 cells were cultured at 1×10^5 cells/well on chitosan and 10% (w/w) HA incorporated HA/chitosan composite scaffolds, TCP, and latex. The 24-well cell culture plate containing samples was then incubated at 37°C in an atmosphere of 5% CO_2. After 1-week period of culture, cell morphology and cell viability were evaluated via SEM and live/dead assay, respectively. No living cells were observed on the surface of latex plates under the fluorescence microscope, indicating that latex was cytotoxic. Although the well of the cell culture plate was not removable and the cell culture plate was too high to focus on the cells seeded on its bottom (TCP) using the fluorescence microscope, the cells seeded on TCP were still visualized using an inverted optical microscope and grown into a confluent state. After 7 days of culture, morphology of L929 cells adhering to HA/chitosan scaffolds was shown
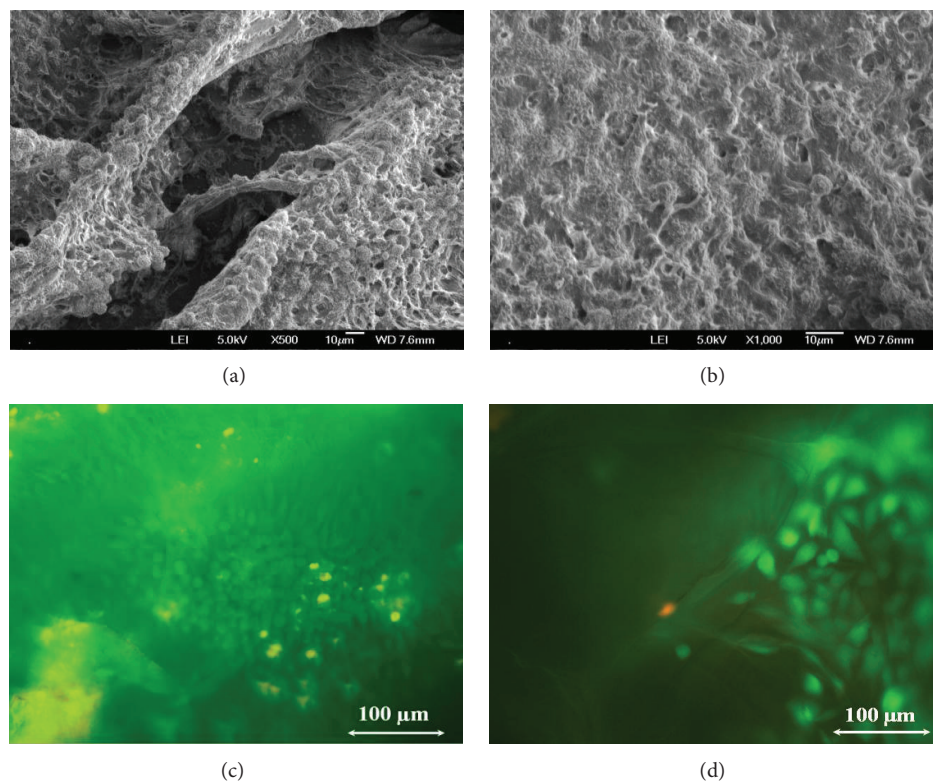
FIGURE 8: ((a), (b)) SEM micrograph and ((c), (d)) fluorescence image of HA/chitosan scaffolds surface cultured for 7 days with fibroblast-like cells.

in Figures 8(a) and 8(b). Similar to those seeded on TCP, L929 cells on the composite scaffolds had grown into a confluent state to form a monolayer. Additionally, most of L929 cells exhibited a round morphology on the surface of HA/chitosan scaffolds, while a few cells were elongated and showed a typical spindle-like morphology inside the porous structure. On the cell surface, many nodules were also observed. Similarly, results from fluorescence images were consistent with the SEM observation. Moreover, the live/dead assay showed that more than 95% cells adhering to HA/chitosan scaffolds were viable and metabolically active (Figures 8(c) and 8(d)), indicating that most of cells on the composite scaffold are still living at day 7. The cell viability of the composite scaffold was calculated according to the fluorescence images. Cell viability was calculated by counting the number of live cells as well as dead cells and then dividing the number of live cells by the number of total cells in the fluorescence images. At least 7 areas were randomly chosen for the cell viability assessment. By means of the similar method used in the investigation, Billiet reported that more than 97% of HepG2 cells were viable after being cultured on 3D printing of gelatin methacrylamide scaffolds for 7 days [25]. Therefore, the cell viability of the composite scaffold (95%) indicated the cytocompatibility of the HA/chitosan scaffolds.

It was reported that a chitosan (CS)/hydroxyapatite (HA) nanohybrid scaffold was prepared by using thermally induced phase separation with a pore size of about 100–136 μm [26]. Improvement of the compressive modulus and good *in vitro*

bioactivity of the nanohybrid scaffold was also reported. In the current study, HA nanoparticles were synthesized separately and then this HA nanoparticles was incorporated into the composite scaffolds. In this study, we have reported not only the compressive properties but also other properties like degradation properties and *in vitro* cell culture results. These two properties are crucial for the scaffolds to be used as tissue engineering scaffolds.

4. Conclusions

The chitosan and HA/chitosan composite scaffolds were successfully fabricated using thermally induced phase separation technique. By varying the materials and processing parameters, degree of porosity and pore sizes of the scaffolds could be modulated. The scaffolds were highly porous and exhibited interconnected porous structure with pore sizes from 20 μm to 350 μm. HA nanoparticles were successfully incorporated which reduced the initial water uptake properties of the scaffolds and also enhanced compressive mechanical properties. Biodegradable and biocompatible porous scaffolds were demonstrated to be suitable for *in vitro* cell culture and are expected to allow cell attachment and tissue in-growth when used *in vivo*.

Conflict of Interests

The authors, hereby, declare that they do not have any conflict of interests.

Acknowledgments

References

[1] R. P. Lanza, R. S. Langer, and J. Vacanti, *Principles of Tissue Engineering*, Elsevier / Academic Press, Amsterdam, The Netherlands, 3rd edition, 2007.

[2] L. G. Griffith and G. Naughton, "Tissue engineering—current challenges and expanding opportunities," *Science*, vol. 295, no. 5557, pp. 1009–1014, 2002.

[3] A. Atala and R. P. Lanza, *Methods of Tissue Engineering*, Academic Press, San Diego, Calif, USA, 2002.

[4] S. J. Hollister, "Porous scaffold design for tissue engineering," *Nature Materials*, vol. 4, no. 7, pp. 518–524, 2005.

[5] Y. Khan, M. J. Yaszemski, A. G. Mikos, and C. T. Laurencin, "Tissue engineering of bone: material and matrix considerations," *Journal of Bone and Joint Surgery A*, vol. 90, no. 1, pp. 36–42, 2008.

[6] P. X. Ma, "Scaffolds for tissue fabrication," *Materials Today*, vol. 7, no. 5, pp. 30–40, 2004.

[7] V. J. Chen and P. X. Ma, "Scaffolding in tissue engineering," P. X. Ma and J. H. Elisseeff, Eds., Taylor & Francis, Boca Raton, Fla, USA, 2005.

[8] J. Han, Z. Zhou, R. Yin, D. Yang, and J. Nie, "Alginate-chitosan/hydroxyapatite polyelectrolyte complex porous scaffolds: preparation and characterization," *International Journal of Biological Macromolecules*, vol. 46, no. 2, pp. 199–205, 2010.

[9] H.-D. Wu, J.-C. Yang, T. Tsai et al., "Development of a chitosan-polyglutamate based injectable polyelectrolyte complex scaffold," *Carbohydrate Polymers*, vol. 85, no. 2, pp. 318–324, 2011.

[10] P. J. Vandevord, H. W. T. Matthew, S. P. Desilva, L. Mayton, B. Wu, and P. H. Wooley, "Evaluation of the biocompatibility of a chitosan scaffold in mice," *Journal of Biomedical Materials Research*, vol. 59, no. 3, pp. 585–590, 2002.

[11] M. Rinaudo, "Chitin and chitosan: properties and applications," *Progress in Polymer Science*, vol. 31, no. 7, pp. 603–632, 2006.

[12] H.-D. Wu, D.-Y. Ji, W.-J. Chang, J.-C. Yang, and S.-Y. Lee, "Chitosan-based polyelectrolyte complex scaffolds with antibacterial properties for treating dental bone defects," *Materials Science and Engineering C*, vol. 32, no. 2, pp. 207–214, 2012.

[13] J. B. Park and J. D. Bronzino, *Biomaterials: Principles and Applications*, CRC Press, Boca Raton, Fla, USA, 2003.

[14] B. D. Ratner, *BioMaterials Science: An Introduction to Materials in Medicine*, Elsevier Academic Press, London, UK, 2nd edition, 2004.

[15] N. Sultana and T. H. Khan, "*In vitro* degradation of PHBV scaffolds and nHA/PHBV composite scaffolds containing hydroxyapatite nanoparticles for bone tissue engineering," *Journal of Nanomaterials*, vol. 2012, Article ID 190950, 12 pages, 2012.

[16] H.-W. Tong, M. Wang, Z.-Y. Li, and W. W. Lu, "Electrospinning, characterization and in vitro biological evaluation of nanocomposite fibers containing carbonated hydroxyapatite nanoparticles," *Biomedical Materials*, vol. 5, no. 5, Article ID 054111, 2010.

[17] W. Y. Zhou, M. Wang, W. L. Cheung, B. C. Guo, and D. M. Jia, "Synthesis of carbonated hydroxyapatite nanospheres through nanoemulsion," *Journal of Materials Science*, vol. 19, no. 1, pp. 103–110, 2008.

[18] Y.-Y. Hsu, J. D. Gresser, D. J. Trantolo, C. M. Lyons, P. R. Gangadharam, and D. L. Wise, "Effect of polymer foam morphology and density on kinetics of in vitro controlled release of isoniazid from compressed foam matrices," *Journal of Biomedical Materials Research*, vol. 35, no. 1, pp. 107–116, 1997.

[19] N. Sultana and T. H. Khan, "Factorial study of compressive mechanical properties and primary in vitro osteoblast response of PHBV/PLLA scaffolds," *Journal of Nanomaterials*, vol. 2012, Article ID 656914, 8 pages, 2012.

[20] T. Sun, L.-P. Wang, and M. Wang, "(Ti, O)/Ti and (Ti, O, N)/Ti composite coatings fabricated via PIIID for the medical application of NiTi shape memory alloy," *Journal of Biomedical Materials Research B*, vol. 96, no. 2, pp. 249–260, 2011.

[21] N. Sultana and M. Wang, "PHBV/PLLA-based composite scaffolds fabricated using an emulsion freezing/freeze-drying technique for bone tissue engineering: surface modification and in vitro biological evaluation," *Biofabrication*, vol. 4, no. 1, Article ID 015003, 2012.

[22] C. Schugens, V. Maquet, C. Grandfils, R. Jerome, and P. Teyssie, "Biodegradable and macroporous polylactide implants for cell transplantation: 1. preparation of macroporous polylactide supports by solid-liquid phase separation," *Polymer*, vol. 37, no. 6, pp. 1027–1038, 1996.

[23] L. J. Gibson and M. F. Ashby, *Cellular Solids: Structure and Properties*, Cambridge University Press, New York, NY, USA, 2nd edition, 1997.

[24] S. Van Vlierberghe, V. Cnudde, B. Masschaele et al., "Porous gelatin cryogels as cell delivery tool in tissue engineering," *Journal of Controlled Release*, vol. 116, no. 2, pp. e95–e98, 2006.

[25] T. Billiet Gevaert E, T. D. Schryver, M. Cornelissen, and P. Dubruel, "The 3D printing of gelatin methacrylamide cell-laden tissue-engineered constructs with high cell viability," *Biomaterials*, vol. 35, no. 1, pp. 49–62, 2014.

[26] J. D. Chen, Y. Wang, and X. Chen, "In situ fabrication of nano-hydroxyapatite in a macroporous chitosan scaffold for tissue engineering," *Journal of Biomaterials Science*, vol. 20, no. 11, pp. 1555–1565, 2009.